Mining of Mineral Deposits
Volume 19 (2025), Issue 3, 120-131

MMD JOURNAL / MINING.IN.UA

https://doi.org/10.33271/mining19.03.120

Real-time deformation monitoring of open-pit mine dump sites using self-developed GNSS receivers: A case study of the Dong Cao Son dump site, Vietnam

Khai Cong Pham [1], Hai Van Nguyen [2*]

[1] *Hanoi University of Mining and Geology, Hanoi, Vietnam*
[2] *Thuyloi University, Hanoi, Vietnam*
**Corresponding author: e-mail haingv@tlu.edu.vn*

Abstract

Purpose. This study aims to develop a real-time deformation monitoring system using GNSS/Continuously Operating Reference Station (CORS) technology for open-pit mine dump sites.

Methods. The system comprises a single CORS station installed in Cam Pha City, Quang Ninh Province, Vietnam, utilizing a Stonex GNSS receiver and a Trimble Zephyr 2 antenna. Components include a GNSS receiver based on the Trimble OEM BD970 module, monitoring control, and data processing software installed on a server computer for remote access. The real-time kinematic (RTK) method using CORS technology is employed for continuous monitoring at a frequency of 5 Hz, with data output in the standard NMEA format. The sliding window algorithm is applied to detect displacement occurrences and magnitudes. Performance and reliability are evaluated through two experiments with varying baseline lengths.

Findings. The simulation experiment results show a maximum difference of 5 mm in horizontal displacement and 8 mm in vertical displacement when compared with measurements from a laser distance meter. The real-world experiment at the Dong Cao Son waste dump in Quang Ninh Province, Vietnam, confirms the system's effectiveness and feasibility. Monitoring data are successfully transmitted to a host computer at Hanoi University of Mining and Geology.

Originality. This study introduces a novel real-time deformation monitoring system based on GNSS/CORS technology, designed to ensure continuous, stable operation and real-time data processing over extended periods.

Practical implications. The developed system provides an efficient, economical, and safe solution for real-time monitoring and early warning of deformations at open-pit dump sites, contributing to improved mining operations.

Keywords: *GNSS, CORS, mine dump deformation, open-pit mine, sliding window, Dong Cao Son dump*

1. Introduction

Landslides are a common natural hazard in mountainous regions with steep slopes and in mining areas. A landslide is the movement of a mass of soil. It rocks down a slope under the influence of gravity, along with other contributing factors such as surface and groundwater pressure, seismic tectonic, and human activities [1]. Landslides often damage property and human lives, destroy structures at the base of waste dumps, and cause environmental degradation [2]. Since waste dumps are artificial landforms created during the mineral extraction, landslides, displacements, and deformations continuously occur from the initial dumping phase and can persist for many years thereafter. To minimize the geographical area used, mining waste is typically dumped in a designated area following a specific method or sequence, with a natural slope angle and usually at a height significantly greater than the original terrain.

After blasting, excavation, and transportation, the soil and rock in the waste dump become loose and lack the cohesive strength they had in their undisturbed state. These conditions are reinforced by rainfall, causing the soil and rock in waste dumps to be prone to displacement. Literary research indicated that the soil and rock in waste dumps continuously displace, causing surface deformation [3]. The intensity of displacement and deformation is most incredible during the initial dumping phase and gradually decreases over time. Real-time monitoring of displacement and landslides in waste dumps provides highly valuable information, such as the movement's magnitude, velocity, and direction. This information helps us understand how the displacement evolves and enables early warnings about the potential occurrence of future landslides.

One of the strategies to mitigate risks caused by landslides is the implementation of real-time monitoring and immediate warning systems. Various solutions have been proposed for monitoring landslides utilizing a system of sensors embedded in the sliding mass [4]-[6], total stations [7], terrestrial laser scanners [8], and remote sensing techniques [9], [10]. The application of Global Positioning System (GPS) technology for monitoring landslides and

Received: 13 January 2025. Accepted: 18 September 2025. Available online: 30 September 2025

Mining of Mineral Deposits. ISSN 2415-3443 (Online) | ISSN 2415-3435 (Print)

other geological hazards has been documented in research studies [11]-[14], indicating its effectiveness. Each of the aforementioned methods has its advantages, disadvantages, and applicability. These methods operate based on discrete monitoring periods; therefore, the monitoring data is not continuous, making it impossible to provide early warning of landslides.

Since the advent of Global Navigation Satellite System (GNSS) technology, many countries have established Continuously Operating Reference Stations (CORS) networks as spatial infrastructure for various purposes, including landslide monitoring. The advantage of CORS networks is continuous operation in all weather conditions, providing real-time correction in the three dimensions [15]. The application of CORS networks with the Virtual Reference Station (VRS) technique has been used for real-time landslide monitoring [16]. The benefit of using a CORS network is that it allows for large distances between CORS and tracking stations, thereby reducing the number of required stations and lowering monitoring costs. However, the CORS network technology is influenced significantly by atmospheric errors, such as ionospheric and tropospheric delays, which limit the positioning accuracy of the VRS technique to approximately the centimeter level [17].

In addition to CORS network technology, single CORS technology combined with low-cost GNSS receivers has also been studied in various works [18]-[20]. The advantage of single CORS technology is its ability to better eliminate the influence of atmospheric errors on monitoring results. However, single CORS technology has limitations, such as the restricted distance between the CORS and monitoring stations, which increases the number of CORS stations, leading to higher monitoring costs. CORS stations are also prone to displacement and unstable geological masses. Additionally, low-cost GNSS receivers are used, resulting in lower accuracy and inefficient data transmission.

Some of Vietnam's largest open-pit coal mines are concentrated in the Cam Pha region of Quang Ninh Province. Millions of cubic meters of soil and rock are excavated annually and dumped into waste piles. Among these, the Dong Cao Son waste dump is the largest in Vietnam, covering an area of over 452 hectares, with the height of the waste dump approximately 300 meters above sea level. Given the location and height, the likelihood of landslides and the displacement of soil and rock is very high. However, landslide and displacement monitoring at the Dong Cao Son waste dump are still based on periodic measurements using traditional surveying equipment, such as levels, electronic total stations, and GPS receivers. Currently, the Vietnam Department of Surveying, Mapping, and Geographic Information has completed the construction of the CORS network (called VNGEONET) of 65 stations across the entire territory of Vietnam. However, this station density is still low, with large distances between stations, ranging from 80 to 120 km, making it challenging to apply the CORS network with VRS techniques for monitoring displacement and landslides at open-pit mine waste dumps.

Therefore, this study aims to apply single CORS technology as a reference station and to develop a high-precision GNSS receiver for monitoring displacement and landslides at waste dumps in open-pit mines in Vietnam.

2. Methods

A method for real-time detection of displacement and landslides at waste dumps in open-pit mines is proposed, which includes a GNSS-based monitoring system and processing and analyzing the monitoring data.

2.1. The monitoring system

2.1.1. Design of the GNSS-based displacement monitoring system

The GNSS-based monitoring system for displacement and landslides must be designed to ensure stable and continuous operation, signal decoding, data transmission, processing, and real-time display. The system consists of three main components, shown in Figure 1. The first component is the single CORS station, the second is the network of monitoring stations, and the third is the data transmission system.

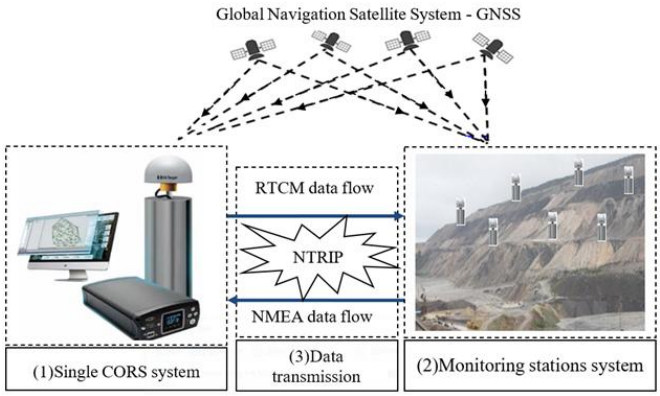

Figure 1. Diagram of the landslide monitoring system based on single CORS technology

The single CORS system provides positional correction to the monitoring stations in the standard Radio Technical Commission for Maritime Services (RTCM) format. It processes the data of RTK measurement networks, corrects integer ambiguities of the CORS system, and develops correction models for tropospheric, ionospheric, and satellite orbit errors. Additionally, the CORS station's central computer hosts the data processing software for the CORS station, monitoring data processing software, and serves as a data storage center. The monitoring station system consists of multiple GNSS receivers using the RTK relative method. The GNSS receivers connect with the CORS station's central computer via a 4G WiFi modem and receive positional corrections from the CORS station to obtain accurate coordinates. The corrected coordinates of the monitoring stations are transmitted to the main computer in the standard NMEA format.

The data transmission system is responsible for transmitting positional corrections from the CORS station to the monitoring stations and transmitting the data from the monitoring stations to the main computer of the CORS station. Data is transmitted using the Network Transport of RTCM via Internet Protocol (NTRIP). The monitoring system operates based on the GNSS relative positioning method, utilizing carrier-phase and pseudorange measurements. To eliminate or minimize specific error sources affecting positioning results, differencing equations (phase differences) are employed. The second-order differencing equations of the CORS station, the monitoring station, and two satellites i and j eliminate satellite and receiver clock errors and, therefore,

are commonly used to determine the baseline vector. The second-order differencing equations for pseudorange and carrier-phase measurements are [21]:

$$\left.\begin{aligned} \Delta\nabla P_{MC}^{i,j} &= \Delta\nabla\rho_{MC}^{i,j} + \Delta\nabla I_{MC}^{i,j} + \Delta\nabla T_{MC}^{i,j} + \Delta\nabla\varepsilon_P \\ \lambda.\Delta\nabla\phi_{MC}^{i,j} &= \Delta\nabla\rho_{MC}^{i,j} - \Delta\nabla I_{MC}^{i,j} + \Delta\nabla T_{MC}^{i,j} - \lambda.\Delta\nabla N_{MC}^{i,j} + \Delta\nabla\varepsilon_\phi \end{aligned}\right\}, \quad (1)$$

where:

$\Delta\nabla$ – the second-order difference, i and j are the non-reference and the reference satellites;

M, C – the monitoring and the CORS stations;

P, ϕ – the pseudorange and the carrier-phase measurements;

λ – the carrier wavelength;

ρ – the geometric distance between the monitoring and CORS stations to the satellites;

I – the ionospheric delay;

T – the tropospheric delay;

N – the integer ambiguity;

ε_P – the random pseudorange noise and other errors.

Additionally, in relative positioning, minimizing errors caused by tropospheric and ionospheric delays is necessary. These errors have a spatial correlation with the baseline length; therefore, to reduce their impact on RTK positioning, the baseline length should not exceed 10 km.

2.1.2. Establishment of the CORS station system

The main components of a CORS station are the GNSS CORS antenna and receiver. In addition, there are several auxiliary components, such as data transmission cables, internet connection and modem, server computer, power supply, and uninterruptible power supply (UPS).

The antenna used in the CORS station must be designed to ensure high phase center stability, eliminate multipath errors, improve measurement accuracy, and provide the best positioning solutions by receiving satellite signals within the GNSS system. This study uses a Zephyr 2 Trimble geodetic receiver (USA). The Zephyr 2 geodetic antenna fully supports the reception of current and future GNSS satellite signals, including GPS, GLONASS, Galileo, BeiDou, QZSS, IRNSS, OmniSTAR, Trimble RTX, and SBAS [22].

The GNSS receiver used in the CORS station is the Stonex SC2000 receiver (Italy). The SC2000 receiver offers high accuracy, robust performance, and stability. It can receive signals from 555 channels of satellites in the GNSS constellation, determine coordinates using carrier-phase measurements with an accuracy of less than 1mm, and support data linking through 4G telecommunication networks, Bluetooth, and WLAN. It can be easily configured via WebUI and remote computers and supports the NTRIP server and NTRIP Caster. The accuracy for static measurements is 3 mm + 0.1 ppm in the horizontal and 3.5 mm + 0.4 ppm in the vertical. The accuracy for RTK measurements is 8 mm + 1 ppm in the horizontal and 15 mm + 1 ppm in the vertical [23].

The GNSS antenna is installed on a pillar that has been surveyed and selected in accordance with technical standards, ensuring it is securely and stably constructed. The GNSS CORS antenna is located in Cam Pha City, Quang Ninh Province, Vietnam, within 10 km of the Dong Cao Son waste dump. The Zephyr 2 geodetic antenna is connected to the SC2000 GNSS receiver via a specialized cable. The receiver is linked to a WiFi modem with internet connectivity and is powered by a stable power supply. Data from the SC2000 GNSS receiver is transmitted to the main server computer set up at the Hanoi University of Mining and Geology.

2.1.3. Determination of the coordinates of the CORS station

The coordinates of the CPCOC6 station are adjusted using the Trimble Business Center 5.2 (TBC 5.2) software and connected to several nearby CORS stations in the VNGEONET network (Fig. 2). The input data in the Rinex format used in the adjustment are obtained from the CORS station over an observation duration of 48 hours.

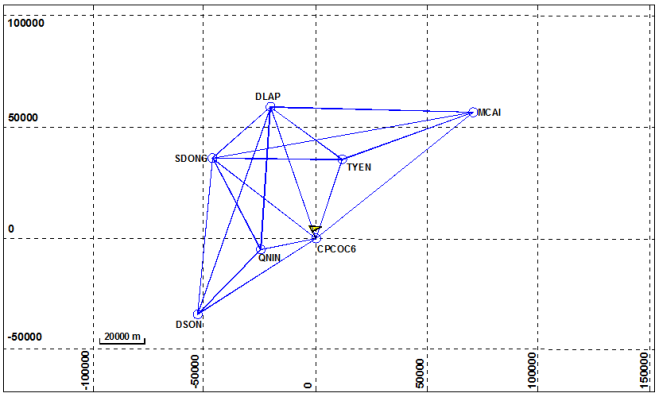

Figure 2. Diagram of the CAMPHA Network after baseline solution

The coordinates of the CORS station CPCOC6 after adjustment in the geocentric Cartesian coordinate system and their root mean square error are shown in Table 1. The coordinates of the CPCOC6 station are input to the GNSS SC2000 receiver via the WebUI (User Interface) by logging into the receiver through the Internet Explorer browser and entering the IP address: 192.168.1.8.

2.1.4. Design of the components of the real-time monitoring system

We design the real-time monitoring system of displacement and landslide of waste rock dumps with components shown in Figure 3.

The name and features of each component in the real-time monitoring system of displacement and landslides of waste rock dumps are shown in Table 2.

Table 1. Geocentric Cartesian coordinates of CORS stations after adjustment

No.	Station	Components of the geocentric Cartesian coordinate system			RMSE (m)		
		X	Y	Z	m_X	m_Y	m_Z
1	DLAP	-1745598.78725	5672891.65324	2327550.26809	0.00092	0.00071	0.00259
2	DSON	-1724387.01504	5714538.80995	2239949.35580	0.00093	0.00070	0.00261
3	MCAI	-1832589.78244	5646288.92354	2324879.29953	0.00095	0.00072	0.00286
4	QNIN	-1748220.88257	5696376.11332	2267426.69992	0.00094	0.00070	0.00268
5	SDON	-1722819.93506	5688541.30127	2306007.29293	0.00090	0.00068	0.00247
6	TYEN	-1779027.03634	5671511.54804	2305159.56917	0.00087	0.00067	0.00238
7	CPCOC6	-1771161.81800	5687390.41800	2272073.82000	0.00280	0.00220	0.01510

Table 2. Name and features of each component in the monitoring system

No.	Component	Feature	Note
1	GNSS antenna	Receiving GNSS signal	Supplied by the manufacturer
2	GNSS receiver	Receiving and decoding GNSS signals	Self-developed
3	WiFi modem with 4G SIM card	Transmission of monitoring data	Supplied by the manufacturer
4	Alarm and signaling module	Warning through sound and lighting	Supplied by the manufacturer
5	12V battery	Storage and supplying power for the GNSS receiver and modem	Supplied by the manufacturer
6	Solar energy-charged controller	Charging the battery	Supplied by the manufacturer
7	Solar panel	Providing input power for the monitoring station system	Supplied by the manufacturer

Figure 3. Components and their connection diagram in the real-time landslide and displacement monitoring station system: 1 – GNSS antenna; 2 – GNSS receiver; 3 – WiFi modem with 4G SIM card; 4 – alarm and signaling module; 5 – 12V battery; 6 – solar energy-charged controller; 7 – solar panel

2.1.5. Design and development of the GNSS receiver for the monitoring station

The GNSS receiver is designed and developed based on the Trimble OEM BD970 module (Fig. 4a). This module can receive 220 channels from satellite systems, such as GPS (L1C/A, L2E, L2C, L5), GLONASS (L1C/A, L1P, L2C/A, L2P), SBAS (L1C/A, L5), Galileo (L1BOC, E5A, E5B, E5AltBOC1), BeiDou (B1, B2), and QZSS (L1C/A, L1 SAIF, L2C, L5). The RTK positioning accuracy is 8 mm + 1 ppm in the horizontal component and 15 mm + 1 ppm in the vertical component, with a baseline of up to 30 km [24].

This module has an Ethernet LAN port. It can be connected to a WiFi modem to transmit monitoring data to the server computer via an IP address and access port on the modem at the CORS station. The GNSS BD970 module, combined with other selected modules, is connected and assembled (Fig. 4b) to form a complete GNSS receiver for the monitoring station system (Fig. 4c).

The GNSS receiver operates using a computer program written in the C# programming language within the Arduino software environment. The program source code is uploaded to the Atmega328P control chip of the GNSS receiver via the Arduino UNO module, which is connected to the computer through a USB port.

The GNSS receiver and other components, as shown in Table 1, form the real-time monitoring station system in Figure 5. This monitoring station system performs high-quality real-time kinematic (RTK) measurements. It transmits the data to the main computer via an IP address and an access port previously configured.

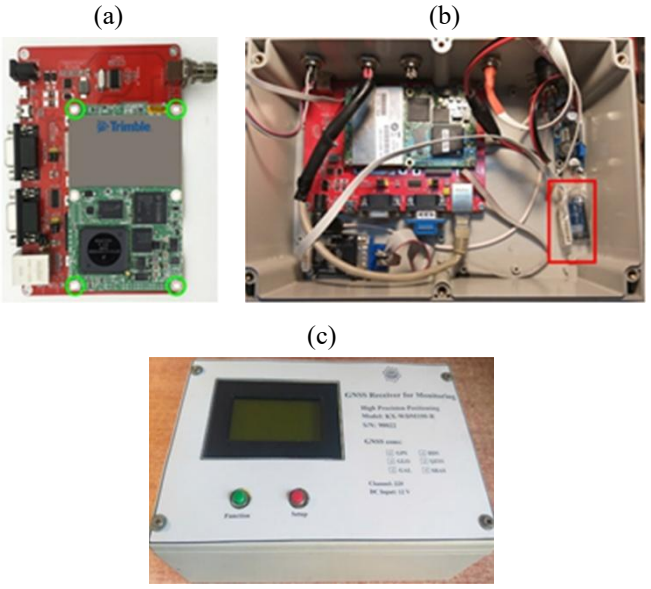

Figure 4. Stages of GNSS receiver station assembly: (a) GNSS receiver module BD970 with Bluetooth and communication components;(b) internal view of the monitoring station during assembly;(c) completed GNSS-based monitoring station with control interface

Figure 5. Real-time landslide monitoring system

2.2. Data processing, analysis, and displacement detection

Data processing, analysis, and displacement detection involve detecting and removing outliers in the RTK time series, converting geocentric Cartesian coordinates to local topocentric coordinates in the WGS84 reference, and analyzing the data to detect displacement.

2.2.1. Outlier detection in RTK time series

In continuous monitoring based on GNSS RTK techniques, outliers may appear alongside points of change caused by sudden displacements. Therefore, during data processing, it is necessary to identify and remove outliers

from the time series. In Figure 6, points I, II, and III are outliers, while point IV is a point of change (also known as a displacement point). Outliers are due to relatively significant deviations in the time series. In contrast, displacement points are caused by changes in state over time within the time series. As shown in Figure 6, after 11:12:15, a change occurred in the measurement time series, and the displacement point was detected.

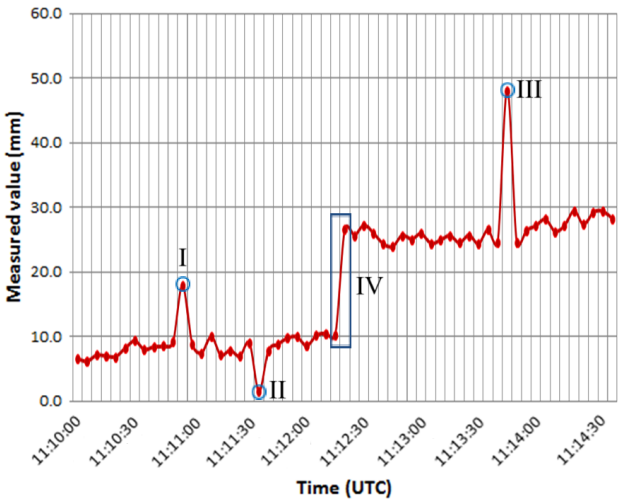

Figure 6. Outlier and displacement points in the time series. I, II, and III are outliers, and IV is the displacement point

Detecting and removing outliers in observational data without accompanying information is challenging, especially with large datasets. To detect outliers in the measurement time series, this study utilizes observational data in the standard NMEA format [25]. NMEA-standard data includes messages of different types. To reduce the size of observational data and ensure more stable data transmission, we use two measurement messages: GGA and GST. These messages contain positional information and other supplementary data, making them suitable for detecting and removing outliers. The GGA message is the most commonly used in GPS or GNSS positioning. It includes the following information: UTC (1), latitude (2), northing (3), longitude (4), easting (5), a quality indicator of positioning (6), the number of satellites used (7), horizontal dilution of precision (8), antenna height above the geoid (9), a unit of antenna height (10), separation between the WGS-84 ellipsoid and the geoid (11), unit of the baseline in meter (12), age of differential GPS data record (13), ID of the reference station, ranging from 0000 to 4095 (14), and checksum of the message string (15). The structure of a GGA message and its details are shown in Figure 7.

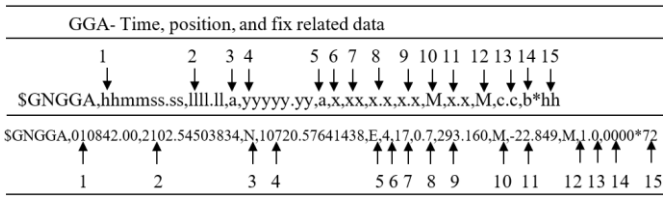

Figure 7. Structure of the GGA message and its details

The GST message contains information about the position correction time (1), residuals of pseudo-range (2), semi-major axis of the error ellipse (3), semi-minor axis of the error ellipse (4), orientation angle of the semi-major axis of the error ellipse (5), error in the *Y*-axis (6), error in the *X*-axis (7), vertical error (8), and the message string checksum (9). The structure of the GST message and its details are shown in Figure 8.

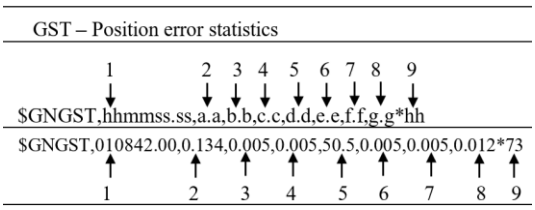

Figure 8. Structure of the GST message and its details

In GGA messages, there is an indicator of the quality of RTK results with six levels numbered from 0 to 5. An indicator of 4 indicates RTK results of high accuracy, and the user will accept this message. Potential outliers are detected based on the following three criteria: completeness of the message series, RTK positioning quality indicator, and the position error. The detection of potential outliers is carried out in the following three steps:

Step 1. Removal of incomplete messages. NMEA-standard messages transmitted from the monitoring station to the central computer via the NTRIP protocol may encounter transmission errors, resulting in incomplete information. To filter out these incomplete messages, their integrity must be verified. The corresponding measurement data lines are discarded if the messages lack complete information. All characters are analyzed from the "$" character to the "*" character to verify the integrity of the information in the measurement message series. Then, a bitwise operation algorithm is applied, starting from the first character to the next, until the end of the series, to generate a new parsed checksum. This parsed checksum is compared with the checksum in the transmitted message. If the two checksums match, the measurement data line is accepted to proceed to the second filtering step.

Step 2. Filtering of position-corrected measurement messages. In RTK positioning, the measurement quality can vary at different levels, which is reflected in the quality indicator in the GGA message. The RTK measurement quality indicator has six levels numbered from 0 to 5. An indicator of 4 corresponds to RTK positioning of the best quality, and the message is retained. Messages with indicators 0, 1, 2, 3, and 5 will be discarded.

Step 3. Filtering of the measurement messages by position errors. The messages with the best quality have been retained after step 2. However, the RTK positioning errors also vary, as shown in the GST message. Only the messages with position errors minor than the allowed limits will be retained to achieve high accuracy. This study uses the horizontal and vertical error limits of 4 and 8 mm. In Figure 6, points I, II, and III are outliers, while point IV is the change point (also known as the displacement point). The outliers are caused by relatively significant deviations in the measurement time series. In contrast, the displacement point is due to a sudden change in the position. As shown in Figure 6, after 11:12:15, a change occurs in the measurement time series, and the displacement point has been detected.

2.2.2. Coordinate conversion

The established monitoring station system uses the RTK dynamic observation method for displacement monitoring. The coordinates of the monitoring station are determined in the geocentric coordinate system with Cartesian components

X, Y, Z or geodetic components B, L, H. For convenience in detecting displacement, these coordinate components, after the three steps of noise filtering mentioned above, will be converted into the local tangent plane coordinate system N, E, U. The relationship between the geocentric Cartesian coordinates and the local tangent plane coordinates is:

$$\begin{bmatrix} N_i \\ E_i \\ U_i \end{bmatrix} = R^T . \begin{bmatrix} X_i - X_o \\ Y_i - Y_o \\ Z_i - Z_o \end{bmatrix}, \quad (2)$$

where:

R^T – the rotation matrix determined as:

$$R^T = \begin{bmatrix} -\sin B_0 \cdot \cos L_0 & -\sin B_0 \cdot \sin L_0 & \cos B_0 \\ -\sin L_0 & \cos L_0 & 0 \\ \cos B_0 \cdot \cos L_0 & \cos B_0 \cdot \sin L_0 & \sin B_0 \end{bmatrix}. \quad (3)$$

The coordinates of the monitoring point in the local tangent plane coordinate system N, E, U are then calculated as:

$$\left.\begin{aligned} N_i &= -(X_i - X_0)\sin B_0 \cos L_0 - (Y_i - Y_0)\sin B_0 \sin L_0 + (Z_i - Z_0)\cos B_0 \\ E_i &= -(X_i - X_0)\sin L_0 + (Y_i - Y_0)\sin L_0 \\ U_i &= (X_i - X_0)\cos B_0 \cos L_0 + (Y_i - Y_0)\cos B_0 \sin L_0 + (Z_i - Z_0)\sin B_0 \end{aligned}\right\}. \quad (6)$$

The horizontal position of the RTK measurement point in the local tangent coordinate system is determined as:

$$P_i = \sqrt{N_i^2 + E_i^2}\ . \quad (7)$$

The observation points' horizontal and vertical position time series (P_i, U_i) are analyzed to detect the horizontal and vertical displacement.

2.2.3 Displacement detection

Real-time displacement detection identifies the time at which the displacement occurs and estimates its magnitude. This study uses the sliding window (SW) model to detect displacement. The SW model is developed based on the Bayesian equation [26] and is interpreted as follows.

Suppose there is a continuous coordinate time series $X(x_1, x_2, \ldots, x_n)$ corresponding to measurement times $T(t_1, t_2, \ldots, t_n)$, referred to as a large array (large window). First, the coordinates time series is split into several smaller arrays (smaller windows) with adjacent sizes typically chosen as $s \geq 5$, depending on the size of the large window. Specifically, the first window starts from the first coordinate to the s^{th} coordinate; the second window starts from the second coordinate to the $(s + 1)^{th}$ coordinate and continues until the X array's end. This approach is called the sliding window method, as shown in Figure 9.

The sliding window method is based on the variation of the standard deviations of the small window (sub-array) within the large window (main array) of coordinates [27].

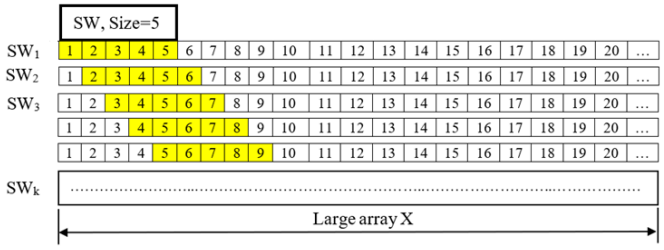

Figure 9. Describe the sliding window method

$$\begin{bmatrix} N_i \\ E_i \\ U_i \end{bmatrix} = \begin{bmatrix} -\sin B_0 \cdot \cos L_0 & -\sin B_0 \cdot \sin L_0 & \cos B_0 \\ -\sin L_0 & \cos L_0 & 0 \\ \cos B_0 \cdot \cos L_0 & \cos B_0 \cdot \sin L_0 & \sin B_0 \end{bmatrix} \cdot \begin{bmatrix} X_i - X_0 \\ Y_i - Y_0 \\ Z_i - Z_0 \end{bmatrix}, \quad (4)$$

where:

B_0, L_0, H_0 – the geodetic coordinates of the origin point of the local tangent plane coordinate system;

X_0, Y_0, Z_0 – the geocentric Cartesian coordinates of the origin point calculated as:

$$\left.\begin{aligned} X_0 &= (N_0 + H_0)\cdot \cos B_0 \cdot \cos L_0 \\ Y_0 &= (N_0 + H_0)\cdot \cos B_0 \cdot \sin L_0 \\ Z_0 &= \left[N_0\left(1 - e^2\right) + H_0\right]\cdot \sin B_0 \end{aligned}\right\}. \quad (5)$$

For convenience in developing a computer program, the coordinates of the observation point in the local tangent plane coordinate system can be calculated from Equation (3) using Equation (5) as:

Since outliers have been removed previously from the coordinate time series, only displacement points remain. In Figure 8, there are both outliers and displacement points; after outlier removal, only displacement points remain (Fig. 10).

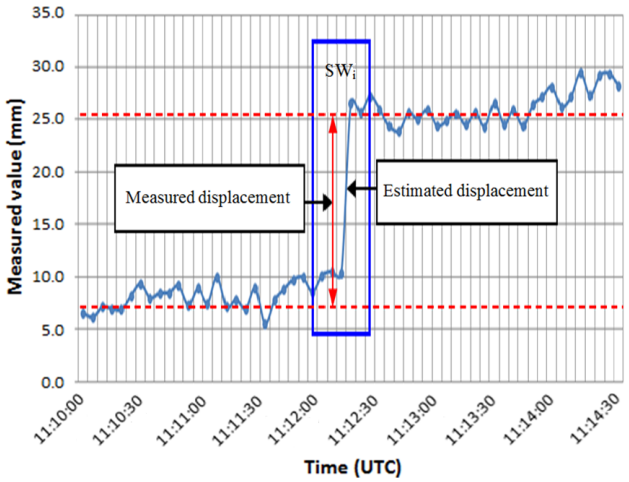

Figure 10. Displacement points in a coordinate time series after outlier removal

After selecting the size of the sliding window, the standard deviation of the i^{th} window is computed as:

$$\sigma_i = \sqrt{\frac{\sum_{j=1}^{n}\left(x_j - \overline{x_i}\right)^2}{s-1}}, \quad (8)$$

where:

x_j – the j^{th} observation;

i – the sliding window index;

$\overline{x_i}$ – the mean value in the i^{th} window;

s – the window size.

The number of sliding windows with a size s in the time series of k observations is calculated as:

$$nsw = k - s + 1 . \quad (9)$$

To detect the displacement points, a threshold value of 3σ is used. This threshold is used as:

$$\left\{ \begin{array}{l} \left| x_j - \bar{x}_i \right| \le 3\sigma \rightarrow Non-displacement\ x_j\ point \\ \left| x_j - \bar{x}_i \right| \ge 3\sigma \rightarrow Displacement\ x_j\ point \end{array} \right\}. \quad (10)$$

The estimated displacement value will be calculated as the difference between the measurement value of the last point and its preceding point in the sliding window in which the displacement occurs:

$$Q_{est} = x_j - x_{j-1} . \quad (11)$$

The estimated displacement is:

$$Q_m = \frac{1}{n_2} \sum_{k=n_1+1}^{n_2} x_k - \frac{1}{n_1} \sum_{i=1}^{n_1} x_i . \quad (12)$$

Suppose there is an RTK measurement time series as shown in Figure 10, consisting of 57 measurement points after outlier removal. If the sliding window size is 15, then the number of sliding windows is 44. The calculation results for detecting displacement points with an RTK measurement time series are shown in Table 3.

Table 3. Example calculation results of displacement points detection

nsw	Time UTC	$\left\|x_j - \bar{x}_i\right\|$	σ, mm	3σ, mm	The last observation in the window	Q_{est}, mm	Q_m, mm	Note
1	11:11:10	2.07	1.12	3.37	10.0	–	–	
2	11:11:15	0.85	1.08	3.25	7.1	–	–	
3	11:11:20	0.23	0.96	2.89	7.9	–	–	
…	……..	……..	……..	……..	……	–	–	
14	11:12:15	1.64	1.49	4.47	10.3	–	–	
15	11:12:20	16.71	4.85	14.54	26.6	16.3	18.0	displacement point
…	……..	……..	……..	……..	……	–	–	
…	……..	……..	……..	……..	…….	–	–	
42	11:14:30	2.74	1.65	4.95	29.2	–	–	
43	11:14:35	2.59	1.71	5.14	29.4	–	–	
44	11:14:40	1.31	1.72	5.17	28.3	–	–	

According to Table 3, at sliding window 15, there is a displacement point with $\left|x_j - \bar{x}_i\right| > 3\sigma$ (16.71 > 14.54), and the last point of this window is the displacement point at 11:12:20 (UTC). The estimated displacement is 16.3 mm, while the observed value is 18.0 mm.

2.3. Validation of experimental model

A displacement simulation device is designed and fabricated to verify the proposed monitoring system's feasibility, performance, and accuracy. The simulation device system, shown in Figure 11a, consists of two steel cylindrical tubes of different diameters nested inside each other and positioned vertically. The larger steel tube is fixed, while the smaller one can move vertically inside the larger steel tube to create simulated vertical displacement. A steel circular plate is attached to the top of the smaller steel tube, with a small hole at the center for mounting the GNSS antenna. Three locking pins place the smaller steel tube within the larger steel tube. A metal plate with four small wheels is fixed at the bottom of the larger steel tube. These wheels can move along two horizontal steel bars to create simulated horizontal displacements. A SINCON SD-120C laser distance meter is placed at two fixed reference points to measure horizontal and vertical displacements of the simulation device with an accuracy of ±1 mm. The complete simulation device system is shown in Figure 11b.

Two simulation surveying campaigns were conducted on July 16, 2023, at two locations in Cam Pha City, Quang Ninh Province, Vietnam, as shown in Figure 12. The simulation experiments were carried out with both horizontal and vertical displacements. The GNSS antenna was mounted on the simulation device and connected to the GNSS receiver, implementing the RTK positioning method with the CORS station CPCOC6 via its IP address and access port.

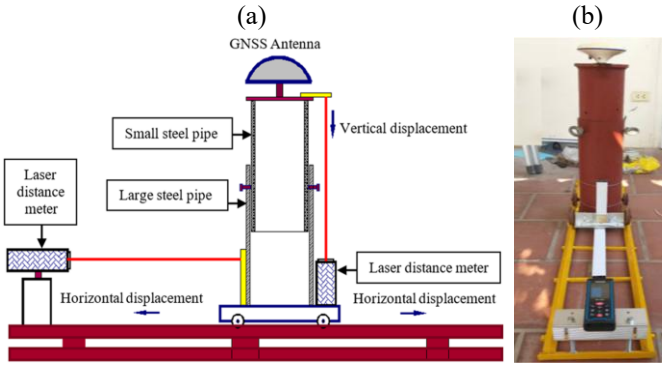

Figure 11. Simulation device used in displacement monitoring: (a) schematic model and detailing parts; (b) real model

In this experiment, six observation cycles were conducted to create five sudden displacements with random values. Each observation was made for approximately 20 minutes, with a signal interval or sampling rate of 5 seconds. After each observation cycle, the antenna's position was changed horizontally and vertically to create simulated displacements. The differences in horizontal and vertical distances from the reference point of the laser distance meter to the antenna's phase center were considered the displacement magnitudes.

The two experimental locations are 3.10 and 11.09 km from the CORS station. The observational data are transmitted to the host computer and saved in a text file. The file name is automatically assigned as the name of the monitoring station, followed by the observation date. Table 4 shows a simulated experimental observation data segment in the standard NMEA format. The observation data are then processed to detect and remove outliers and converted to a local tangent plane coordinate system.

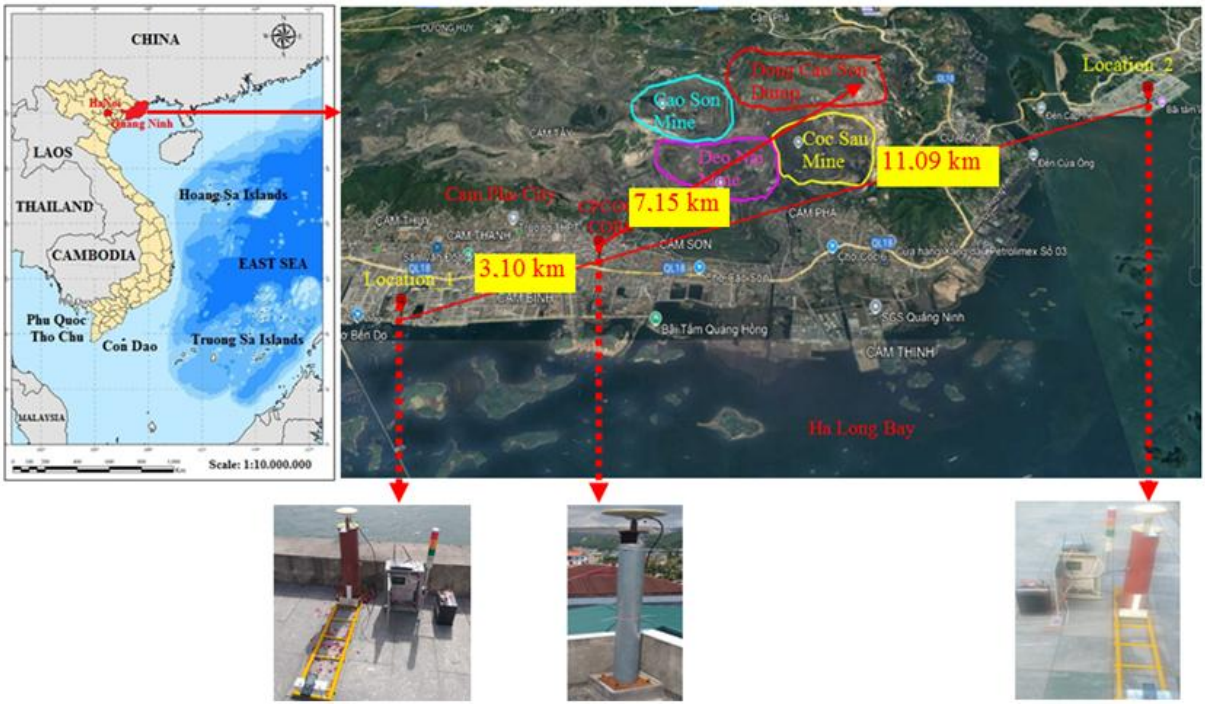

Figure 12. Study areas of simulation and real-world monitoring experiments of mine dump sites in the Google Earth map

Table 4. Coordinates of the monitoring point at different times in a time series after the removal of outliers

No.	Time (UTC)	Geocentric Cartesian coordinates			Local tangent plane coordinates		
		X (m)	*Y* (m)	*Z* (m)	*N* (m)	*E* (m)	*U* (m)
1	04:59:37	-1768531.139	5688654.788	2270997.668	0.000	0.000	0.000
2	04:59:42	-1768531.141	5688654.795	2270997.672	-0.001	0.000	-0.008
3	04:59:47	-1768531.143	5688654.803	2270997.674	0.000	0.001	-0.016
4	04:59:52	-1768531.143	5688654.798	2270997.672	0.000	-0.001	-0.011
5	04:59:57	-1768531.142	5688654.800	2270997.674	-0.002	0.001	-0.013
6	05:00:02	-1768531.141	5688654.798	2270997.671	0.001	0.001	-0.010
7	05:00:07	-1768531.142	5688654.798	2270997.672	0.000	0.000	-0.011
8	05:00:12	-1768531.144	5688654.799	2270997.672	0.001	-0.001	-0.012
9	05:00:17	-1768531.144	5688654.801	2270997.675	-0.001	-0.001	-0.015
10	05:00:22	-1768531.146	5688654.805	2270997.675	0.000	-0.001	-0.013
…	….	……..	…….	…….	…….	…….	…….
1281	07:33:57	-1768531.041	5688654.453	2270998.012	-0.447	-0.005	-0.203
1282	07:34:02	-1768531.041	5688654.449	2270998.008	-0.444	-0.007	-0.208
1283	07:34:07	-1768531.040	5688654.442	2270998.006	-0.445	-0.008	-0.215
1284	07:34:12	-1768531.035	5688654.442	2270998.006	-0.445	-0.004	-0.217
1285	07:34:17	-1768531.038	5688654.438	2270998.005	-0.445	-0.008	-0.220
1286	07:34:22	-1768531.040	5688654.445	2270998.011	-0.448	-0.007	-0.211
1287	07:34:27	-1768531.037	5688654.443	2270998.008	-0.446	-0.005	-0.215
1288	07:34:32	-1768531.038	5688654.447	2270998.009	-0.446	-0.005	-0.211
1289	07:34:37	-1768531.039	5688654.447	2270998.009	-0.445	-0.006	-0.210
1290	07:34:42	-1768531.039	5688654.447	2270998.009	-0.445	-0.006	-0.210

Based on the observation time series coordinates, the observed horizontal and vertical displacements at the first and second locations are detected, as shown in Table 5.

The plots of observed horizontal and vertical displacements from the simulation experiments at the first and second locations are shown in Figure 13.

3. Results and discussion

The real-world field experiment is conducted at the Dong Cao Son waste dump in Cam Pha City, Quang Ninh Province, Vietnam. The Dong Cao Son dump was established to accommodate waste rock disposal from large open-pit mines, including the Cao Sơn, Đèo Nai, and Cọc Sáu mines (Fig. 12). Over the years, the amount of waste rock deposited in this dump has reached hundreds of millions of cubic meters. As per the approved plan, the total surface area of the dump is 636 hectares, with a disposal height of +300 m above sea level. The dump has a length of 3118 m and a width of 1650 m [27]. After decades of operation, meeting the waste disposal needs of open-pit mines in the Cam Pha area, it has become Vietnam's most significant waste dump. A portion of the waste dump has been rehabilitated, restored, and reforested, while most of the area remains active. Due to the large surface area of the dump, the field experiment is conducted in an eastern region with a high potential for displacement. Six monitoring stations were designed within the experimental area and numbered from M1 to M6 (Fig. 14).

Table 5. Results of horizontal and vertical displacements observed from the simulation experiment

Location	Campaign	Time of displacement	Actual displacement (mm)		Observed displacement (mm)		Difference (mm)	
			Horizontal	Vertical	Horizontal	Vertical	Horizontal	Vertical
First location	1	05:21:07	30	-27	25.6	-31.3	4.4	4.3
	2	05:55:12	60	-15	56.2	-20.4	3.8	5.4
	3	06:26:32	73	-30	69.0	-35.5	4.0	5.5
	4	06:47:37	107	-24	102.3	-29.8	4.7	5.8
	5	07:11:52	183	-125	179.5	-129.2	3.5	4.2
Second location	1	08:48:07	49	-68	52.9	-62.4	3.9	5.6
	2	09:14:27	135	-56	140.4	-49.8	5.4	6.2
	3	09:40:37	112	-54	107.1	-48.1	4.9	5.9
	4	10:12:07	108	-43	103.0	-49.5	5.0	6.5

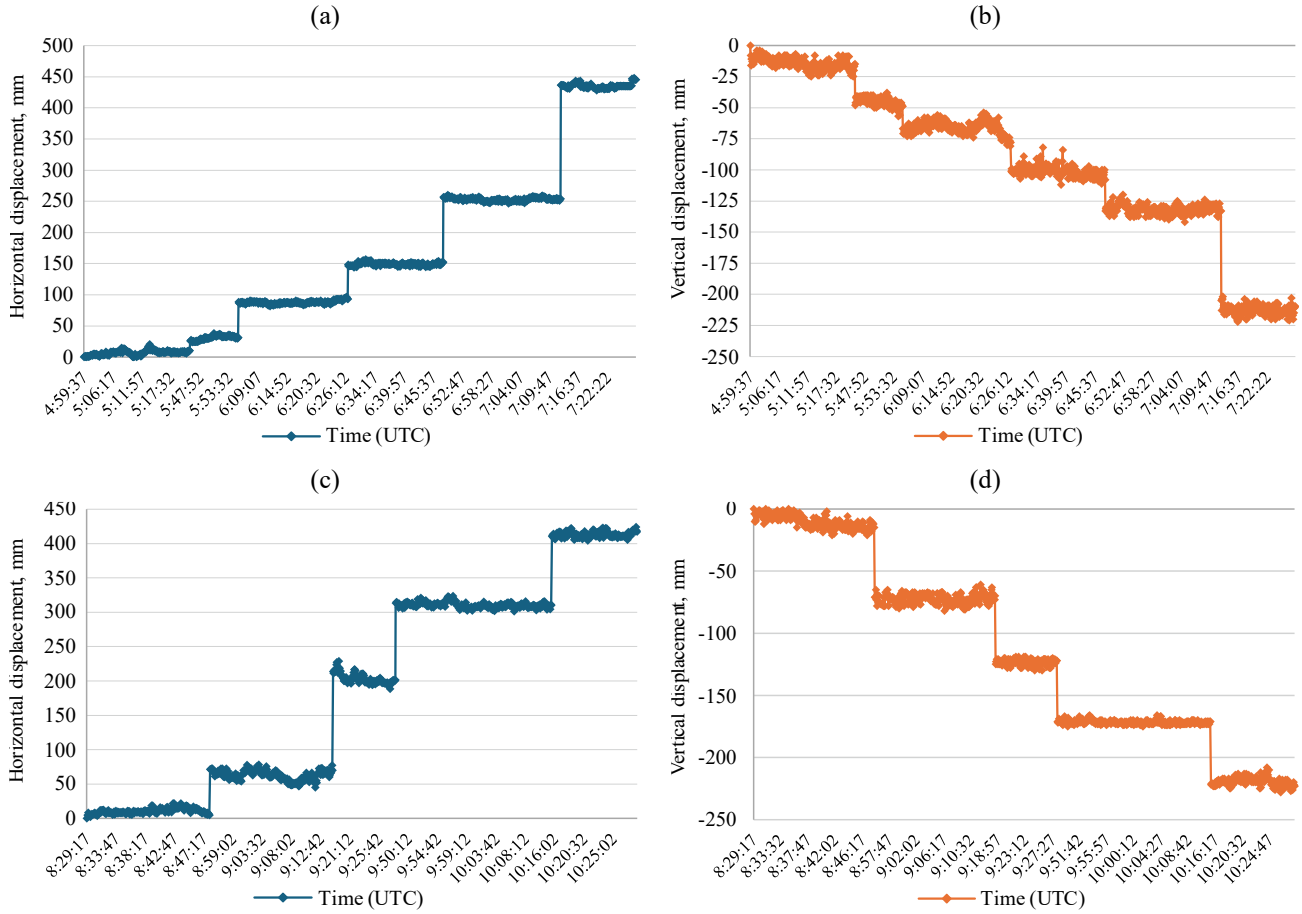

Figure 13. Plots of horizontal and vertical displacements in the simulation experiment: (a) and (b) at the first location; (c) and (d) at the second location

Figure 14. Locations of monitoring points in areas of the Dong Cao Son mining waste dump

At the locations of monitoring stations, reference points are installed deep into the waste dump to monitor the displacement of land and rocks. These reference points are made of pillars on which a secured screw can fix a receiver to reduce receiver centering errors. A 1-meter-long steel cylindrical tube is used to install the antenna of the monitoring station, which is mounted at one end of the cylindrical tube and placed in a secured screw-centering configuration.

Six pillars are designed and fabricated from stainless steel and securely embedded into the waste dump surface using cement mortar at the designated positions. Once the pillars are firmly attached to the surface of the waste dump, the surveying equipment used for the observation station is installed.

After the monitoring station was installed and the parameters were set, it was connected to the CORS station CPCOC6 via the IP address and access port configured in the

CORS station's modem. Data from each monitoring station is transmitted to the main computer located in the laboratory at Hanoi University of Mining and Geology via the IP address 118.70.171.179, with each monitoring station having its own data access port. A computer software package used for observation management, data processing, and analysis, which is termed the GNSS CORS WDM Server, is designed and built, as shown in Figure 15.

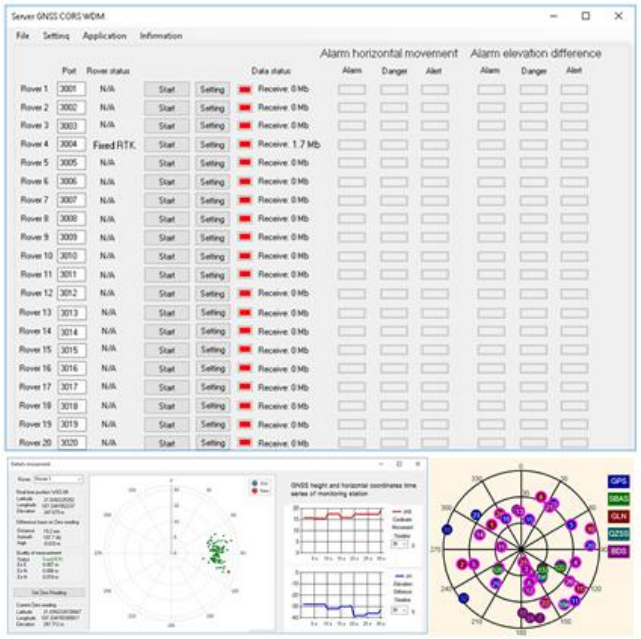

Figure 15. Software interface for real-time monitoring of mining waste dump displacement

This software can manage up to 50 monitoring stations simultaneously, and the data from each station is transmitted to the main computer through its specific access port. Detailed information at each observation station, such as the real-time position of the station, positioning quality, and the point positions time series chart, is displayed on a module of the GNSS CORS WDM Server software. This helps users monitor the real-time movements of the waste dump. In addition, daily data at each observation station in the standard NMEA format are automatically stored in a predefined folder, with the file name created by the station's name followed by the observation date (day, month, year). A segmented processed time series of displacement monitoring of the Dong Cao Son waste dump is shown in Table 6.

The observations were conducted in the two simulated experiments at two different survey station locations with varying baseline distances. At the first location with the baseline distance of 3.10 km to the CORS station CPCOC6, the most considerable differences between the actual and observed displacements were 4.7 mm in the horizontal direction and 5.8 mm in the vertical direction. At the second location with a baseline distance of 11.09 km, the corresponding most significant differences of 5.4 and 6.5 mm in the horizontal and vertical displacements, respectively, were found. The most critical differences observed at the two experimental station locations are shown in Table 7.

As the baseline distance to the CORS station increases, the difference between the actual and observed displacements also increases. This indicates that as the baseline distance increases, the positioning error of the observation station also increases. Therefore, when monitoring displacement at a waste dump site, the baseline distance between the CORS and monitoring stations should not exceed 10 km. In this study, we have established the CORS station CPCOC6 at a distance of 7.5 km from the Dong Cao Son waste dump observation area, which is considered a reasonable distance. The real-time monitoring results of the Dong Cao Son waste dump displacement reflect the actual displacement condition at this site.

Table 6. A segmented processed time series of displacement monitoring of the Dong Cao Son waste dump

No.	Time (UTC)	Geocentric Cartesian coordinates			Local tangent plane coordinates		
		X (m)	*Y* (m)	*Z* (m)	*N* (m)	*E* (m)	*U* (m)
1	1:08:32	-1775322.94	5684896.205	2275884.055	0.000	0.000	0.000
2	1:08:37	-1775322.94	5684896.208	2275884.055	0.002	0.001	-0.003
3	1:08:42	-1775322.941	5684896.209	2275884.058	-0.001	0.001	-0.005
4	1:08:47	-1775322.942	5684896.213	2275884.059	-0.001	0.001	-0.009
5	1:08:52	-1775322.94	5684896.206	2275884.058	-0.002	0.001	-0.002
6	1:08:57	-1775322.935	5684896.204	2275884.058	-0.004	0.005	0.001
7	1:09:02	-1775322.934	5684896.198	2275884.057	-0.004	0.004	0.007
8	1:09:07	-1775322.938	5684896.205	2275884.058	-0.003	0.002	-0.001
9	1:09:12	-1775322.938	5684896.203	2275884.055	0.000	0.002	0.002
10	1:09:17	-1775322.934	5684896.2	2275884.055	-0.002	0.005	0.006
11	1:09:22	-1775322.938	5684896.205	2275884.059	-0.003	0.003	-0.001
12	1:09:27	-1775322.935	5684896.196	2275884.056	-0.004	0.003	0.009
13	1:09:32	-1775322.936	5684896.204	2275884.056	-0.001	0.004	0.002
14	1:09:37	-1775322.939	5684896.205	2275884.056	0.000	0.002	0.000
15	1:09:42	-1775322.935	5684896.2	2275884.052	0.001	0.004	0.007
16	1:09:47	-1775322.935	5684896.199	2275884.053	0.000	0.003	0.007
17	1:09:52	-1775322.936	5684896.198	2275884.054	-0.002	0.002	0.007
18	1:09:57	-1775322.935	5684896.202	2275884.054	0.000	0.004	0.004
19	1:10:02	-1775322.935	5684896.201	2275884.052	0.001	0.004	0.006
20	1:10:07	-1775322.936	5684896.199	2275884.056	-0.003	0.003	0.006
…	….	…….	…….	…….	…….	…….	…….

Table 7. Most significant differences between actual and observed horizontal and vertical displacements at the two simulated experimental locations

Monitoring location	Baseline, km	Largest difference, mm	
		Horizontal	Vertical
First	3.10	4.7	5.8
Second	11.09	5.4	6.5

4. Conclusions

This study has developed a displacement monitoring system in mining waste dumps based on GNSS/CORS technology. A high-precision, low-cost GNSS receiver was developed based on Trimble's technology and was used for real-time displacement monitoring at the waste dumps in open-pit mines. The RTK positioning method provided observation time series for real-time displacement detection. The observation data in the NMEA standard format allowed for real-time data transmission from the monitoring station to the server computer over an IP network using the NTRIP protocol. The observation data in the NMEA standard format were processed through three steps to detect and remove outliers, retaining the highest precision measurements to improve the accuracy of the monitoring results. The outlier-removed observation coordinates were then converted into the local tangent plane coordinate system for displacement analysis. The sliding window model based on the Bayesian equation was developed, successfully detecting the time of displacement occurrence and estimating the displacement magnitude in real time.

The performance of the developed monitoring system was evaluated through two displacement simulation experiments. The maximum differences between actual and measured displacements in the horizontal and vertical directions were 4.7 and 5.8 mm, respectively, when the baseline distance was 3.10 km. With the more extended baseline of 11.09 km, the most significant differences were 5.4 mm for horizontal displacement and 5.8 mm for vertical displacement. The monitoring system has been proven to be entirely feasible for real-time displacement detection at the Dong Cao Son waste dump at open-pit mines in Vietnam.

Author contributions

Conceptualization: KCP; Investigation: KCP, HVN; Methodology: KCP, HVN; Software: KCP, HVN; Writing – original draft: KCP; Writing – review & editing: KCP. All authors have read and agreed to the published version of the manuscript.

Funding

This research received no external funding.

Conflicts of interest

The authors declare no conflict of interest.

Data availability statement

The original contributions presented in the study are included in the article, further inquiries can be directed to the corresponding author.

References

[1] Hu, X., Bürgmann, R., Lu, Z., Handwerger, A.L., Wang, T., & Miao, R. (2019). Mobility, thickness, and hydraulic diffusivity of the slow-moving Monroe landslide in California revealed by L-band satellite radar interferometry. *Journal of Geophysical Research: Solid Earth*, *124*(7), 7504-7518. https://doi.org/10.1029/2019JB017560

[2] Hoy, M., Doan, C.B., Horpibulsuk, S., Suddeepong, A., Udomchai, A., Buritatum, A., Chaiwan, A., Doncommul, P., & Arulrajah, A. (2024). Investigation of a large-scale waste dump failure at the Mae Moh mine in Thailand. *Engineering Geology*, *329*, 107400. https://https://doi.org/10.1016/j.enggeo.2023.107400

[3] Gao, S., Zhou, W., Shi, X., Cai, Q., Crusoe, G. E., Jr., Shu, J., & Huang, Y. (2017). Mechanical properties of material in a mine dump at the Shengli Surface Coal Mine, China. *International Journal of Mining Science and Technology*, *27*(3), 545-550. https://doi.org/10.1016/j.ijmst.2017.03.014

[4] Khoa, V.V., & Takayama, S. (2018). Wireless sensor network in landslide monitoring system with remote data management. *Measurement*, *129*, 214-229. https://doi.org/10.1016/j.measurement.2018.01.002

[5] Georgieva, K., Smarsly, K., König, M., & Law, K.H. (2012). An autonomous landslide monitoring system based on wireless sensor networks. *Computing in Civil Engineering*, *2012*, 0019. https://doi.org/10.1061/9780784412343.0019

[6] Kuang, K.S.C., & Cao, Q. (2015). A low-cost, wireless chemiluminescence-based deformation sensor for soil movement and landslide monitoring. *Structural Health Monitoring*, *2015*, 116. https://doi.org/10.12783/SHM2015/116

[7] Artese, S., & Perrelli, M. (2018). Monitoring a landslide with high accuracy by total station: A DTM-based model to correct for the atmospheric effects. *Geosciences*, *8*(12), 457. https://doi.org/10.3390/geosciences8020046

[8] Gumilar, I., Fattah, A., Abidin, H.Z., Sadarviana, V., Putri, N.S.E., & Kristianto. (2017). Landslide monitoring using terrestrial laser scanner and robotic total station in Rancabali, West Java (Indonesia). *AIP Conference Proceedings*, *1857*, 060001. https://doi.org/10.1063/1.4987084

[9] Liu, Y., Yao, X., Gu, Z., Zhou, Z., Liu, X., & Wei, S. (2024). Study on InSAR image fusion for improved visualization of active landslides in alpine valley areas: A case in the Batang Region, China. *Computers & Geosciences*, *186*, 105481. https://doi.org/10.1016/j.cageo.2023.105481

[10] Strozzi, T., Klimeš, J., Frey, H., Caduff, R., Huggel, C., Wegmüller, U., & Rapre, A.C. (2018). Satellite SAR interferometry for the improved assessment of the state of activity of landslides: A case study from the Cordilleras of Peru. *Remote Sensing of Environment*, *217*, 111-125. https://doi.org/10.1016/j.rse.2018.08.014

[11] Xiao, R., & He, X. (2013). Real-time landslide monitoring of Pubugou hydropower resettlement zone using continuous GPS. *Natural Hazards*, *69*(3), 1647-1660. https://doi.org/10.1007/s11069-013-0768-x

[12] Abidin, H.Z., Andreas, H., Gamal, M., Surono, & Hendrasto, M. (2004). Studying landslide displacements in Megamendung (Indonesia) using GPS survey method. *ITB Journal of Engineering Science*, *36*(2), 109-123. https://doi.org/10.5614/itbj.eng.sci.2004.36.2.2

[13] Su, M.-B., Chen, I.-H., & Liao, C.-H. (2009). Using TDR cables and GPS for landslide monitoring in high mountain area. *Journal of Geotechnical and Geoenvironmental Engineering*, *135*(8), 1113-1121. https://doi.org/10.1061/(ASCE)GT.1943-5606.0000047

[14] Gili, J.A., Corominas, J., & Rius, J. (2000). Using global positioning system techniques in landslide monitoring. *Engineering Geology*, *55*(3), 167-192. https://doi.org/10.1016/S0013-7952(99)00122-1

[15] Zhao, W.Y., Zhang, M.Z., Ma, J., Han, B., Ye, S.Q., & Huang, Z. (2021). Application of CORS in landslide monitoring. *IOP Conference Series: Earth and Environmental Science*, *861*, 042049. https://doi.org/10.1088/1755-1315/861/4/042049

[16] Shu, B., He, Y., Wang, L., Zhang, Q., Li, X., Qu, X., Huang, G., & Qu, W. (2023). Real-time high-precision landslide displacement monitoring based on a GNSS CORS network. *Measurement*, *217*, 113056. https://doi.org/10.1016/j.measurement.2023.113056

[17] Wang, P., Liu, H., Nie, G., Yang, Z., Wu, J., Qian, C., & Shu, B. (2022). Performance evaluation of a real-time high-precision landslide displacement detection algorithm based on GNSS virtual reference station technology. *Measurement*, *199*, 111457. https://doi.org/10.1016/j.measurement.2022.111457

[18] Benoit, L., Briole, P., Martin, O., Thom, C., Malet, J.-P., & Ulrich, P. (2015). Monitoring landslide displacements with the Geocube wireless network of low-cost GPS. *Engineering Geology*, *195*, 111-121. https://doi.org/10.1016/j.enggeo.2015.05.003

[19] Cina, A., & Piras, M. (2015). Performance of low-cost GNSS receiver for landslides monitoring: Test and results. *Geomatics, Natural Hazards and Risk*, *6*(5-7), 497-514. https://doi.org/10.1080/19475705.2014.889046

[20] Bellone, T., Dabove, P., Manzino, A.M., & Taglioretti, C. (2016). Real-time monitoring for fast deformations using GNSS low-cost receivers. *Geomatics, Natural Hazards and Risk*, *7*(2), 458-470. https://doi.org/10.1080/19475705.2014.1003079

[21] Trimble. (n.d.). *Zephyr 2 GNSS antenna [End-of-life product]*. Retrieved from: https://oemgnss.trimble.com/en/products/end-of-life-products/zephyr2
[22] Stonex. (n.d.). *SC2000 GNSS receiver*. Retrieved from: https://www.stonex.it/project/sc2000-gnss-receiver/
[23] Pham, C.K., Tran, D.T., & Nguyen, V.H. (2021). Research and development of real-time high-precision GNSS receivers: A feasible application for surveying and mapping in Vietnam. *Inżynieria Mineralna*, *1*(2(48)), 391-404. https://doi.org/10.29227/IM-2021-02-36
[24] National Marine Electronics Association. (n.d.). *NMEA official website*. Retrieved from: http://www.nmea.org
[25] Shen, N., Chen, L., & Chen, R. (2022). Displacement detection based on Bayesian inference from GNSS kinematic positioning for deformation monitoring. *Mechanical Systems and Signal Processing*, *167*, 108570. https://doi.org/10.1016/j.ymssp.2021.108570
[26] Shehadeh, A., Alshboul, O., & Almasabha, G. (2024). Slope displacement detection in construction: An automated management algorithm for disaster prevention. *Expert Systems with Applications*, *237*, 121505. https://doi.org/10.1016/j.eswa.2023.121505
[27] Pham, C.K., Tran, D.T., & Nguyen, V.H. (2020). GNSS/CORS-based technology for real-time monitoring of landslides on waste dump – A case study at the Deo Nai South Dump, Vietnam. *Inżynieria Mineralna*, *1*(2(46)), 181-191. https://doi.org/10.29227/IM-2020-02-23

Моніторинг деформацій відвалів відкритих гірничих робіт у реальному часі з використанням розроблених GNSS-приймачів: приклад відвалу Донг Као Сон, В'єтнам

К.К. Фам, Х.В. Нгуєн

Мета. Розробка системи моніторингу деформацій у режимі реального часу із використанням технології GNSS/мережі постійно діючих референц-станцій (CORS) для відвалів кар'єрних розробок.

Методика. Система включає єдину CORS-станцію, встановлену у місті Камфа, провінція Куангнінь, В'єтнам, із використанням приймача Stonex GNSS та антени Trimble Zephyr 2. До складу системи входять GNSS-приймач на базі модуля Trimble OEM BD970, програмне забезпечення для контролю моніторингу та обробки даних, інстальоване на серверному комп'ютері для віддаленого доступу. Для безперервного моніторингу застосовується метод кінематики в реальному часі (RTK) на основі технології CORS із частотою 5 Гц, вихідні дані формуються у стандартному форматі NMEA. Для виявлення випадків та величин зміщень використано алгоритм "ковзного вікна". Ефективність та надійність системи оцінювалися за результатами двох експериментів з різною довжиною базової лінії.

Результати. Визначено, що результати модельного експерименту показали максимальну різницю 5 мм для горизонтальних і 8 мм для вертикальних зміщень у порівнянні з альтернативним вимірюванням лазерним далекоміром. Натурний експеримент на відвалі Донг Као Сон у провінції Куангнінь, В'єтнам, підтвердив ефективність і працездатність системи моніторингу деформацій у відвалах кар'єрних розробок. Отримані дані моніторингу деформацій відвалу успішно передані на серверний комп'ютер Гірничо-геологічного університету Ханоя.

Наукова новизна. Представлено нову систему моніторингу деформацій у режимі реального часу на основі технології GNSS/CORS, розроблену для забезпечення безперервної, стабільної роботи та оперативної обробки даних упродовж тривалого періоду.

Практична значимість. Розроблена система є ефективним, економічним і безпечним рішенням для моніторингу в реальному часі та раннього попередження про деформації на відвалах відкритих гірничих робіт, що сприяє підвищенню безпеки та ефективності гірничих операцій.

Ключові слова: *GNSS, CORS, деформація відвалу, відкрите гірниче виробництво, алгоритм ковзного вікна, відвал Донг Као Сон*

Publisher's note

All claims expressed in this manuscript are solely those of the authors and do not necessarily represent those of their affiliated organizations, or those of the publisher, the editors and the reviewers.